








Honey-loaded oral patches: A biocompatible therapeutic potential in accelerating oral mucosal wound healing

SITI NOR NAJIHAH YASIN¹ 
NOOR IZZATI MOKHZANI¹ 
NADIA HALIB¹ 
NORMALIZA AB MALIK² 
MUHAMMAD SYAFIQ ALAUDDIN² 
MOHD RAZIF MOHD IDRIS³ 
ZULFAHMI SAID^{1*} 

¹ Department of Basic Sciences and Oral Biology, Faculty of Dentistry University Sains Islam Malaysia Tower B, Persiaran MPAJ, Jalan Pandan Utama 55100 Pandan Indah, Ampang, Malaysia

² Department of Conservative Dentistry and Prosthodontics Faculty of Dentistry, University Sains Islam Malaysia, Tower B Persiaran MPAJ, Jalan Pandan Utama 55100 Pandan Indah Ampang, Malaysia

³ Pusat Terapi Sel, Tingkat 12, Blok Klinikal, Hospital Canselor Tuanku Muhriz UKM (HCTM), 56000 Cheras, Kuala Lumpur, Malaysia

ABSTRACT

Oral mucosal wound management remains clinically challenging due to continuous exposure to saliva, microbial colonisation, and mechanical stress from mastication and speech. Conventional treatments such as gels and mouthwashes often exhibit short-term relief, resulting in suboptimal therapeutic efficacy. To address these limitations, this study aimed to develop *Tualang* honey (TH)-loaded oral patches for enhanced wound healing. Although TH is widely recognised for its regenerative properties, its incorporation into a sustained-release delivery system for oral tissue engineering remains underexplored. The patches were fabricated using polyvinyl alcohol, sago starch, glycerol, and TH *via* solvent casting, followed by comprehensive physicochemical, mechanical, morphological, and biological evaluations using primary oral fibroblasts. The formulated patches demonstrated uniform surface morphology, satisfactory mechanical strength, and good biocompatibility. Swelling analysis revealed significantly higher water uptake in TH-loaded patches compared to placebo patches. After six months of monitoring, the physicochemical properties of all patches revealed no significant changes, confirming the stability of the formulation. *In vitro* assessments also demonstrated TH-loaded patches enhanced cell viability and accelerated wound closure, highlighting the regenerative properties of TH. Conclusively, TH-loaded patches demonstrated stability, biocompatibility, and improved wound healing *in vitro*, suggesting they could serve as an effective approach for oral mucosal wound management.

Keywords: *Tualang* honey, oral patches, polyvinyl alcohol, sago starch, primary oral fibroblasts

INTRODUCTION

Oral wounds, whether caused by trauma, infections, ulcers, or surgical procedures, are more complex to manage compared to skin wounds (1). The oral cavity has a natural ability to heal rapidly due to high vascularisation and salivary components that support tissue repair (2, 3). However,

continuous exposure to saliva, bacterial colonisation, and mechanical stresses from chewing or swallowing can slow down the healing process, prolong inflammation, and increase the risk of infection (4, 5). This highlights the need for therapeutic strategies that not only protect the wound but also support controlled regeneration.

Drug delivery systems (DDS) technology has gained attention in wound care, as they enable the introduction of therapeutic agents into the body to improve wound recovery (4, 6). Novel drug delivery systems (NDDS) involve various routes of drug administration and are designed to provide minimally invasive and serve better localised, sustained, and controlled drug transportation (5–9). Among different NDDS approaches (ointments, tablets, films, patches, gel forms), hydrogel oral patches provide an alternative to address the deficiencies related to the wound in oral and maxillofacial regions. Oral patch formulations are particularly advantageous because they adhere directly to the wound site, maintain moisture, and provide prolonged protection with reduced need for frequent application (4, 5, 7, 10, 11). Besides functioning as a biological barrier that blocks harmful foreign material from entering the wound, oral patches were also found to effectively prolong drug residence time and prevent overdosing in a short period (4).

The performance of these oral patches largely depends on the choice of polymers, which determine adhesion, biocompatibility, and drug release properties. Recently, the fabrication of patches using natural polymers has become the focus of research. Natural polymers, specifically sago starch, are widely used because they are non-toxic, affordable, sustainable, and biocompatible, making them suitable for wound-healing applications. However, some limitations, such as low mechanical strength and a lack of hydrophilicity, make this polymer unable to stand alone in fabricating patches (12). Meanwhile, various synthetic polymers have also been used in wound-healing applications. Among them, polyvinyl alcohol (PVA) is highly recognised among researchers as it possesses biocompatible, biodegradable, non-carcinogenic, water-soluble, low interfacial tension, and high swelling ratio properties that offer better functionality and mechanical strength, which can be tailored to meet the problem (10, 12). Therefore, by pairing both types of polymers, this hybridisation allows improvements in stability, durability, and control of degradation rate properties (13).

Recently, the addition of natural bioactive agents, such as honey, has been explored to enhance the healing potential of these systems further. *Tualang* honey (TH), in particular, has demonstrated antimicrobial, anti-inflammatory, and tissue-regenerative effects (14–16), making it a strong candidate for oral wound therapy. Previous studies on honey-based gels and films also showed improved healing outcomes compared to conventional treatments (17). Based on these considerations, this study focuses on developing a *Tualang* honey-loaded oral patch comprising PVA, sago starch and TH. The aim is to combine the benefits of a localised NDDS with the therapeutic properties of TH to accelerate epithelial regeneration, reduce microbial contamination, and provide an effective non-invasive treatment for oral wound healing. Furthermore, comprehensive studies regarding oral patch formulations combining PVA, sago starch and TH are scarce, thereby reinforcing the significance of this study.

EXPERIMENTAL

Materials

Sago starch powder (brand Cap Bintang), manufactured by THC Sdn Bhd, was obtained from Healthy Living Organic (organic store). Polyvinyl alcohol (PVA) (Ph Eur,

ChP, USP, JPE grade, 85.0–89.0 % hydrolysis, 4.3–5.7 mPa s viscosity) and glycerol were supplied by Merck (UK) and Sigma-Aldrich (UK), respectively. Distilled water was used as a solvent to prepare the solutions. Pure *Tualang* honey with the brand An-Nahlu was purchased from An-Nahlu Supplier Trading (herbal medical store). For biological testing, primary oral fibroblasts (POF) derived from human gingival tissue were purchased from ATCC Primary Cell Solutions (USA) with ATCC number PCS-201-018.

Chemical characterisation and identification of Tualang honey

The chemical characterisation, identification and chemical quantitation of the TH was certified by UNIPEQ, UKM (Malaysia). The analysis involves ash content, moisture content, sugar content (fructose, glucose, maltose, sucrose), hydroxymethylfurfural (HMF) content, pH, and free acidity. The methodology and results certificate can be referred to Appendix 1 (available upon request).

Formulation of Tualang honey-loaded oral patches

Oral patches were prepared using the solvent-casting method. A 5 % (*m/V*) sago starch dispersion was prepared by dispersing 5 g of sago starch in 100 mL of distilled water, followed by heating at 75–80 °C under continuous stirring until complete gelatinisation occurred, resulting in the formation of a viscous gel-like texture. Concurrently, a 10 % (*m/V*) PVA solution was prepared by dissolving 10 g of PVA powder in 100 mL of distilled water at 80 °C. Sago starch and PVA solution were mixed at a 3:7 (*V/V*) ratio with the addition of 2.5 % (*w/V*) of glycerol. The mixture was homogenised for 1 hour, cooled to room temperature, and then blended with 2 mL of diluted *Tualang* honey (TH) at concentrations of 0.19, 0.39, 0.78, 1.56, and 3.12 % (*V/V*) relative to the total formulation volume, followed by stirring for another 1 hour. After that, the mixture was gently poured into approximately 20 mL or ½ Petri dish and allowed to evaporate and dry for 72 h at room temperature. The patch must be solidified and can be lifted from the Petri dishes before being cut into 2 × 1 cm pieces and stored until further use. This formulation was also the same for the placebo patch (without TH) group.

Patches characterisation

Scanning electron microscopy analysis. – The microstructure of the surface and the interface of the oral patches was evaluated using Scanning Electron Microscopy (SEM). The placebo and selected TH-loaded patches (0.39 and 3.12 %TH) were adhered to a 1 × 1 cm piece of carbon tape attached to the metallic stubs (10 mm). All samples were sputter-coated with gold, and images of the patch's surface were captured at 5 kV using scanning electron microscopy (JEOL, Germany).

Physicochemical analysis. – This study examined the physicochemical characteristics of oral patches: mass, thickness, and pH. The placebo and TH-loaded patches were measured using an electronic digital balance and a digital micrometre for mass and thickness, respectively. As for pH, the placebo and TH-loaded patches were immersed in 5 mL of distilled water for 30 minutes before testing the pH with a pH-meter (Mettler Toledo, US).

Mechanical properties analysis. – The folding endurance and tensile strength of oral patches were analysed functionally to assess their flexibility and durability. For folding properties, the placebo and TH-loaded patches were mechanically folded at the same spot

until they broke or at least folded up to 350 times manually, as it was considered a suitable property for good patches. For the tensile strength analysis, the placebo and TH-loaded patches were mounted in the grips with a gauge length of 25 mm. The samples were then stretched using a tensile tester (TA. XTplus Texture Analyzer, UK) with a motor speed of 8.30 mm s^{-1} . All parameters were performed in triplicate, and each sample was tested three times.

Swelling index analysis. – For this analysis, the initial mass of the placebo and TH-loaded patches was weighed (m_0) using an electronic digital balance, followed by immersion in 5 mL of distilled water at predetermined intervals of 5, 10, 15, 20, 30, and 40 minutes. After that, the patches were removed from the solution and were blotted with Whatman filter paper to remove excess water before being weighed for the final reading (m_i). The difference in masses between m_0 and m_i due to absorption and swelling was then calculated and normalised to the initial mass (m_0) before being multiplied by 100 to express the degree of swelling index as a percentage (Equation 1):

$$\text{Swelling index (\%)} = [(m_i - m_0) / m_0] \times 100 \quad (1)$$

Stability analysis. – The placebo and TH-loaded patches were subjected to short-term stability testing. Therefore, biodegradability testing was used to observe the condition of the patches at room temperature over six months. Changes in the characteristics of the stored patches were investigated after storage at the end of last month.

Biological characterisation

Cell cytotoxicity analysis. – The toxicology of TH, sago starch, and TH-loaded patches was analysed using the MTT assay (MTT = 3-(4,5-dimethylthiazol-2-yl)-2,5-diphenyl-2H-tetrazolium bromide) on a primary oral human cell line, primary oral fibroblasts (POF). Briefly, for toxicology analysis of TH, POF cells were seeded at a density of 1.0×10^4 cells per well in 100 μL per well of Dulbecco's Modified Eagle's Medium (DMEM), in a 96-well plate and incubated in 95 % air and 5 % CO_2 at 37°C for 24 hours. After incubation, the media was discarded and replenished by 100 μL per well culture medium containing various percentage of TH (0.09, 0.19, 0.39, 0.78, 1.56, 3.12, 6.25, 12.5, 25, 50 and 100 %) which make 12 groups of treatment including control group and subsequently incubated in a time-dependent manner (24, 48 and 72 h). After incubation, the treatment medium was discarded, and the cells were washed before exposure to $0.5 \mu\text{g mL}^{-1}$ MTT solution for 2 hours. After that, 50 μL of DMSO was added to solubilise the blue formazan, and the absorbance (OD value) of the sample was measured using a microplate reader (SpectraMax[®] iD3, Software, California) at 570 nm, with a 630 nm reference correction. The data were then expressed as cell viability percentages. The same procedure was done to test the toxicology of sago starch. The percentage of the starch remains the same as TH: 0.09, 0.19, 0.39, 0.78, 1.56, 3.12, 6.25, 12.5, 25, 50 and 100 % (m/V). To achieve the concentrations, sago starch was weighed and diluted in 100 mL of sterile distilled water, then filtered before treating the cells.

For oral patch toxicology, the placebo and TH-loaded patches were sterilised using UV light for 10 minutes. Then, each sample was incubated in DMEM at 37°C overnight until it dissolved, after which the solutions were filtered. Concurrently, POF cells were seeded in a 96-well plate at 1.0×10^4 cells per well in 100 μL DMEM and incubated in 95 % air and

5 % CO₂ at 37 °C for 24 hours. After incubation, the media was discarded and replaced with 100 µL per well filtered solution of patches, and the plates were incubated at 37 °C in 5 % CO₂ for 3 different periods (24, 48, and 72 h). After incubation, the treatment medium was discarded, and the cells were washed before exposure to 0.5 µg mL⁻¹ MTT solution for 2 h. After that, 50 µL of DMSO was added to solubilise the blue formazan. Finally, the absorbance (OD value of the sample) was measured in a microplate reader (SpectraMax® iD3, Software, USA) at 570 nm, with a 630 nm reference correction. The cell viability was then expressed as a percentage relative to the untreated control group by dividing the OD value of the sample by the OD value of the control before multiplying the value by 100 using Equation 2:

$$\text{Cell viability (\%)} = (\text{OD}_{\text{sample}} / \text{OD}_{\text{control}}) \times 100 \quad (2)$$

Scratch wound healing analysis. – For wound healing properties, oral patches were tested *in vitro* using two-dimensional (2D) models. Briefly, the placebo and selected TH-loaded patches (3.12 %) were sterile for wound closure analysis, as confirmed by UV light for 10 minutes. Then, each sample was incubated in DMEM at 37 °C overnight until it dissolved, after which the solution was filtered. Concurrently, POF cells were seeded at 2×10^4 cells per well in 2 mL DMEM into a 12-well plate and incubated overnight at 37 °C in 5 % CO₂. After overnight incubation, the culture medium was discarded, and the monolayer cells were scratched with three perpendicular lines using a sterile 200 µL pipette tip. The 12-well plate was filled with 2 mL DMEM as the control group (without the oral patch), and with 2 mL of the filtered patch solutions for the placebo group and the 3.12 % TH group. The diameter of the wound and the image migration of cells in the scratch area of each well were observed under an inverted microscope (Olympus BX51, Germany), and were recorded at 0, 24, 48, and 72 h, respectively. The data were presented as the percentage of wound closure, calculated based on the reduction in the mean wound width. The average of multiple horizontal distances measured at 0 hours (D_0) was subtracted from the average of multiple horizontal distances measured at the selected time point (D_t), normalised to the initial wound width and multiplied by 100 using Equation 3:

$$\text{Wound closure (\%)} = [(D_0 - D_t) / D_0] \times 100 \quad (3)$$

Each value represents the mean of at least three independent measurements across the wound area.

Statistical analysis

The data from this study were statistically analysed using the Statistical Package for the Social Sciences (SPSS) for Windows, version 25.0 (SPSS Inc., USA), and reported as mean ± SD. Statistical significance was analysed using one-way analysis of variance (ANOVA) and was considered significant when $p < 0.05$.

RESULTS AND DISCUSSION

Characterisation of oral patches structure

Scanning Electron Microscopy (SEM) analysis was performed to analyse the surface and cross-sectional morphology of placebo and TH-loaded patches (Fig. 1). The SEM analysis

showed that both the placebo and TH-loaded patches exhibited irregularities and a rougher top surface. The cross-sections of both patches further confirmed that the rough surface may be attributed to the distribution of clumping molecules, which may result from starch agglomeration.

The selection of starch molecules at a lower ratio, specifically below 10 %, was highly recommended for patch formulation (18, 19), as it offers a balanced combination and is characterised by non-toxicity, low immunogenicity, cost-effectiveness, and natural degradation without harmful residues (20, 21). However, agglomeration might occur due to exchange temperature during preparation (22, 23).

Concurrently, the addition of TH also increases surface roughness, as the irregularities increase with its high ratio. Apart from that, honey agglomeration might occur due to strong hydrogen-bond interactions between TH particles and the polymer network, specifically PVA, during temperature changes during solvent evaporation (24). Nevertheless, the roughness characteristic was reported not to affect drug release (25) and, at the same time, to contribute to swelling properties, as the rough surface enhanced the surface area for fluid absorption (26, 27). This characteristic is particularly beneficial for wound healing applications, as it provides a larger surface area, allowing the patch to absorb exudates while maintaining a moist environment conducive to tissue regeneration (28, 29).

Overall, the SEM analysis demonstrated that incorporating TH into the patches resulted in desirable morphological properties, including enhanced surface roughness and a denser internal structure. These characteristics align with the requirements for effective oral patches, as they contribute to improved adhesion (30), enhanced fluid absorp-

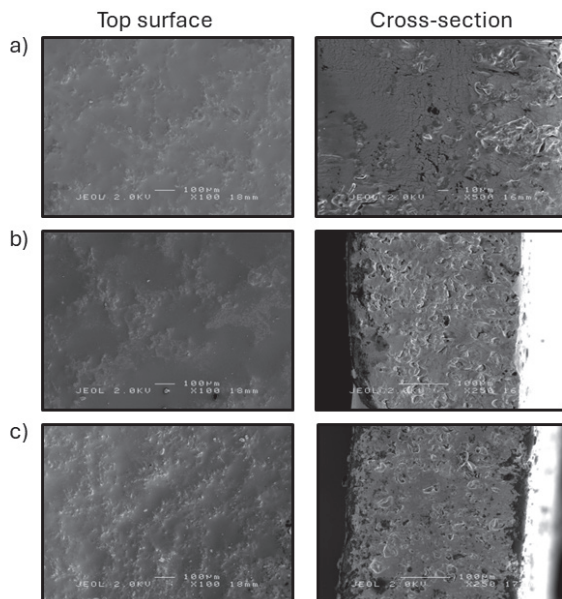


Fig. 1. SEM images of oral patches with different percentages of *Tualang* honey: a) 0 % (placebo); b) 0.39 % TH; c) 3.12 % TH taken at 100 \times (scale bar = 100 μ m) (SEM – scanning electron microscope, TH – *Tualang* honey).

tion (28), and greater structural durability (29). Therefore, future optimisation of the formulation process, such as controlling the honey cooling rate (31) and improving starch dispersion techniques (32), could further refine the morphology of the patches for enhanced therapeutic performance.

Physicochemical characterisation of oral patches

The physicochemical properties of the patches were assessed using three analyses: mass, thickness, and pH. When incorporating a few concentrations of *Tualang* honey (TH) (0.19, 0.39, 0.78, 1.56, and 3.12 %) in the oral patch, there are no significant changes ($p > 0.05$) in the mass value as TH-loaded patches were recorded with 0.114 ± 0.020 g to 0.150 ± 0.031 g compared to the placebo patches with 0.133 ± 0.026 g (Fig. 2a). Similar to thickness, the presence of TH somehow does not interfere with the thickness value, as the thickness recorded was in a range between 0.372 ± 0.002 mm to 0.459 ± 0.004 mm. In contrast, the placebo patch thickness was 0.391 ± 0.009 mm (Fig. 2b). However, for pH value, the presence of TH influenced the value as it fell into a range between 5.984 ± 0.050 and 7.231 ± 0.057 , decreasing as the honey concentration increased, compared to placebo patch that was almost neutral (pH 7.65 ± 0.097) (Fig. 2c).

The mass and thickness properties of oral patches are critical parameters that influence the uniformity of drug content, stability, and the release mechanism during the application. When both placebo and TH-loaded patches exhibit a non-significant difference, this indicates the consistent reproducibility across batches by using the solvent-casting method. To maintain consistency, the solvent-casting method was an effective choice, as it has been shown to allow precise control over the thickness, composition, and cohesive properties of gellan gum-pectin films and polyvinyl alcohol-chitosan hydrogels (33, 34). According to previous studies, the ideal average thickness of the patches that demonstrated rapid drug release was between 0.1 and 0.5 mm (35–37). Since the thickness of the oral patches ranged from 0.372 ± 0.002 mm to 0.459 ± 0.004 mm, within the ideal range, this formulation ensured adequate comfort during adhesion to the oral mucosa, avoiding excessive bulkiness that could interfere with speaking or chewing.

The higher thickness observed in the placebo may be attributed to the higher effective polymer network density between PVA and sago starch, resulting in increased polymer solid content per unit volume (13) compared to TH-loaded patches. The incorporation of TH at a lower ratio likely disrupted the polymer-polymer hydrogen bonding due to its sugar and higher water content, resulting in thinner films. Interestingly, patches loaded with 3.12 % TH, showed a slight increase in thickness compared to placebo, which may be associated with the higher sugar content in the TH contributing to increased solid mass and potential conformation rearrangement within the polymer networking between sugar, starch and PVA molecules, leading to the slight swelling and conformational changes. This was in line with previous studies, in which hydrophilic additives, such as honey, increased patch thickness and mass due to their dense molecular structure and high solids content, which help retain moisture and disrupt compact polymer packing (10, 34). However, since the increment showed no significant deviation compared to the placebo, this suggests that incorporating TH into the formulation maintains homogeneity and produces consistent patches suitable for oral wound-healing applications.

The incorporation of TH resulted in a concentration-dependent reduction in pH, with values ranging from 7.231 ± 0.057 to 5.984 ± 0.050 . A gradual decrease in pH value was observed

with increasing TH ratio, with the lowest value (5.984 ± 0.050) recorded in patches incorporated with 100 % TH. According to previous studies, changes in pH corresponded to the honey's natural pH, reported as 3.55 to 4.00 (20, 38). This suggests that slightly acidic environments aid in suppressing bacterial growth and enhancing oxygen release, which are crucial

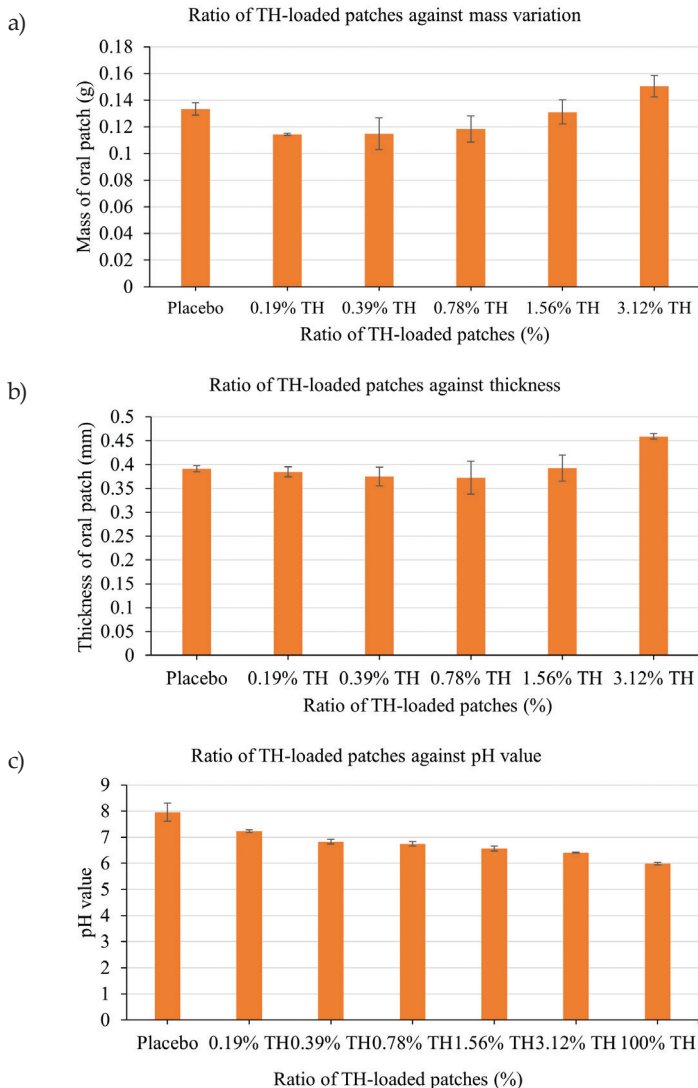


Fig. 2. Placebo and TH-loaded patches (0.19, 0.39, 0.78, 1.56 and 3.12 %) are characterised for a) mass; b) thickness and c) pH value with three different batches. Data are presented as the mean \pm SD from three independent experiments. Each was performed in triplicate, and $p < 0.05$ was considered significant compared to the placebo group (TH – Tualang honey, SD – standard deviation).

for the tissue repair process (39). Since the pH of TH-loaded patches falls within the pH range of the physiological oral mucosa (5.5–7.6) (40), this suggests that incorporating TH can maintain the balance of the oral mucosa during healing and prevent mucosal irritation.

Mechanical characterisation of oral patches

The mechanical characterisation of the patches was assessed through folding endurance and tensile strength analysis to evaluate their flexibility and resilience, and to determine their resistance to mechanical stress that could lead to breakage. Based on the result, the incorporation of TH inside the formulation showed no significant increases ($p > 0.05$) in the folding endurance with value 389 ± 2.60 to 485.667 ± 1.986 compared to placebo patches with 366.111 ± 6.819 (Fig. 3a). Similar to tensile strength, the addition of TH does not significantly interfere ($p > 0.05$) the tensile strength as the result showed that TH-loaded patches exhibited slightly higher tensile strength with value 0.215 ± 0.012 MPa when exposed to 1.56 % TH-loaded patches while the lowest tensile strength exhibit by 3.12 % TH-loaded patches with value 0.166 ± 0.016 MPa compared to placebo patches 0.168 ± 0.003 MPa (Fig. 3b).

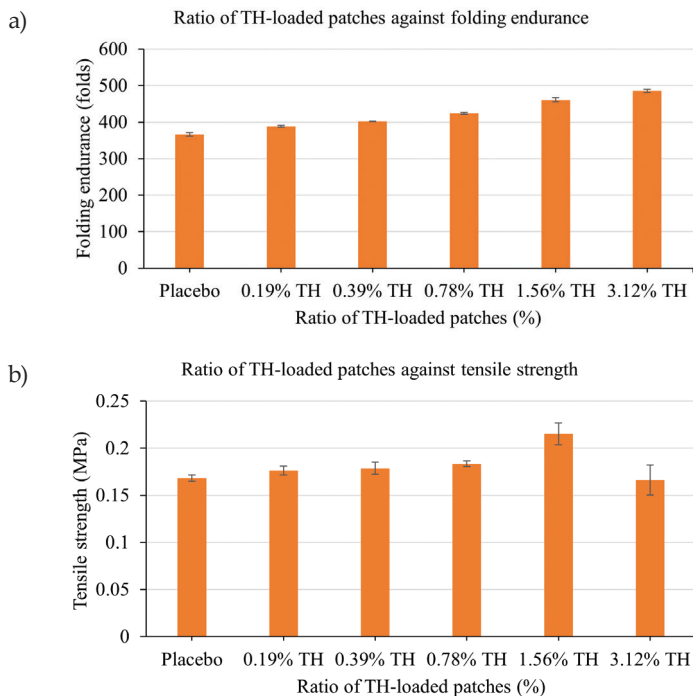


Fig. 3. Placebo and TH-loaded patches (0.19, 0.39, 0.78, 1.56 and 3.12 %) are characterised for: a) folding endurance; b) tensile strength with three different batches. Data are presented as the mean \pm SD from three independent experiments. Each was performed in triplicate, and $p < 0.05$ was considered significant compared to the placebo group (TH – *Tualang* honey, SD – standard deviation).

Mechanical characteristics are crucial properties that need to be studied to create durable, resilient patches for use during oral movements such as speaking and chewing (41). The presence of TH in oral patches resulted in greater endurance and tensile strength than placebo patches, suggesting a stronger interaction between TH and polymer molecules within the patches. This finding aligned with a previous study, which found that the presence of honey can enhance hydrogen bonding between biopolymers and active compounds, leading to stronger integrity of the composition (42). Besides, the data pattern is also in line with the exposure of the Manuka honey-sodium alginate hydrogel film at a lower ratio, specifically 2 %, which exhibited the highest tensile strength (43). *Vice versa*, the highest ratio of Manuka honey-sodium alginate hydrogel film (10 %) shows the lowest tensile strength. According to the same study, although a higher honey ratio indicates stronger hydrogen bonding, solution concentration still affects stickiness, which, in turn, affects tensile stress and strain values.

On the other hand, this oral patch formulation also showed folding endurance values exceeding 350 folds for both placebo and TH-loaded patches, indicating that the patches maintained their structure without breaking. This might be attributed to the addition of the plasticiser, glycerol, which functionally enhances flexibility and prevents brittleness in the formulation (44, 45). Therefore, combining TH and glycerol in the formulation suggests an optimised balance of strength and flexibility, making it suitable for prolonged mucosal adhesion in the oral region .

Swelling index of oral patches

The swelling index used in this study was designed to evaluate a patch's absorption and moisture retention over a specific period of time. From Fig. 4, the results show that the percentage of swelling index increased with increasing immersion duration. The presence

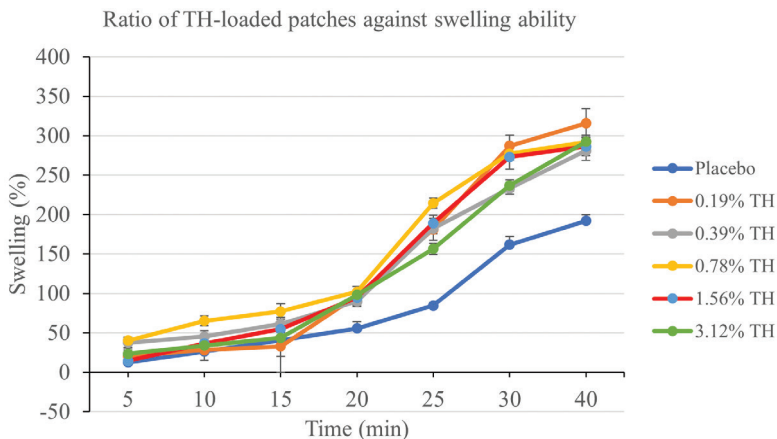


Fig. 4. Placebo and TH-loaded patches (0.19, 0.39, 0.78, 1.56 and 3.12 %) are characterised by swelling index ratio across three different batches. Data are presented as the mean \pm SD from three independent experiments. Each was performed in triplicate, and $p < 0.05$ was considered significant compared to the placebo group (TH – *Tualang* honey, SD – standard deviation).

of TH specifically at concentration 0.78 %, shows significantly highest rate of swelling index in minutes 5 until minutes 25 of immersion compared to other groups with value 40.232 ± 4.526 % to 214.453 ± 6.232 %, while in minutes 30 and 40, the significant highest percentage were shown by 0.19 % TH-loaded patches with value of 287 ± 13.255 % and 315.709 ± 18.561 % respectively. For TH-loaded patches at 0.39 % concentration, swelling was higher after 5–15 minutes, but at 20 minutes or more, it decreased compared to other concentrations. Apart from that, for TH-loaded patches with concentrations above 0.78 % (1.56 % TH and 3.12 % TH), the swelling ability was lowest but slightly higher than that of placebo patches.

Swelling properties are an essential characteristic of oral patches, as they determine absorption capacity, adhesion, and drug release (46–48). From the result, TH exhibited a higher swelling percentage than placebo patches, indicating that TH has a greater capacity to enhance the moisture retention of the patches (49). This might be attributed to the TH's hygroscopic nature, which enhanced the fluid absorption by attracting and retaining moisture from the environment into the patches (50, 51). Since the incorporation of TH enhanced the moisture-retaining capacity of the patches, this may create an optimal environment for healing, drug delivery, and patient comfort.

Stability of oral patches

Stability analysis comprising mass, thickness, pH, folding endurance, and colour change parameters was evaluated for 1, 3, and 6 months, and the data were tabulated in Table I. Across all parameters, no significant changes were observed during the time interval. The results show that all parameters, such as weight, thickness, pH value, and folding endurance, were maintained for 6 months. The colour of the patches also remains the same over the time interval observed with the naked eye, indicating their stability under controlled storage conditions. These findings suggest that the patches can retain their therapeutic efficacy and physical properties over extended storage periods, making them suitable for commercialising as an alternative oral healing application.

Cell cytotoxicity analysis and biocompatibility of oral patches

Toxicology analysis was conducted on primary oral fibroblasts (POF) using 0.5 mg mL^{-1} of MTT to assess cell metabolic activity at various concentrations of TH, starch and TH-loaded patches. Exposure of POF cells to TH showed a non-significant increase ($p > 0.05$) in percentage viability at concentrations below 0.78 % TH. It was noted that the percentage viability of POF cells at concentrations 0.09 % TH (100.126 ± 6.649 %), 0.19 % TH (110.828 ± 5.953 %), 0.39 % TH (111.868 ± 8.418 %) and 0.78 % TH (106.711 ± 8.214 %) was above 100 % when culturing for 24 hours, compared to the control group. After 48 h of exposure, only treatments with 0.09 % TH (101.584 ± 3.960 %) and 0.19 % TH (101.577 ± 2.108 %) showed increased percentage viability. The same holds for the 72-hour treatment; only the 0.09 % and 0.19 % TH concentrations showed higher viability, with values of 112.453 ± 8.636 % and 114.568 ± 2.279 %, respectively, compared to the control. At concentrations above 0.78 % TH, POF cells exhibited a time-dose-dependent reduction in viability, with viability dropping sharply at 6.25 % TH (Fig. 5a).

Table I. Stability testing data for the placebo and TH-loaded patches (0.19, 0.39, 0.78, 1.56 and 3.12 %)

Patch	Time interval (months)	Test parameter ^a (Mean ± SD) (n = 9)				Colour changes
		Mass (g)	Thickness (mm)	pH	Folding endurance (folds)	
Placebo	0	0.139 ± 0.001	0.397 ± 0.010	8.21 ± 0.07	371.67 ± 4.50	No
	1	0.133 ± 0.026	0.393 ± 0.029	8.27 ± 0.05	366.33 ± 8.45	
	3	0.133 ± 0.001	0.391 ± 0.009	8.26 ± 0.06	366.11 ± 6.82	
	6	0.128 ± 0.001	0.383 ± 0.014	8.27 ± 0.05	360.33 ± 7.50	
0.19 % TH	0	0.115 ± 0.002	0.397 ± 0.010	7.23 ± 0.06	391.67 ± 1.03	No
	1	0.115 ± 0.001	0.384 ± 0.004	7.30 ± 0.11	389.00 ± 2.56	
	3	0.115 ± 0.009	0.383 ± 0.019	7.24 ± 0.07	389.00 ± 0.89	
	6	0.113 ± 0.003	0.373 ± 0.019	7.21 ± 0.02	386.33 ± 5.75	
0.39 % TH	0	0.129 ± 0.004	0.460 ± 0.018	6.83 ± 0.09	404.33 ± 3.14	No
	1	0.115 ± 0.026	0.400 ± 0.003	6.84 ± 0.01	404.00 ± 4.73	
	3	0.112 ± 0.003	0.363 ± 0.010	6.86 ± 0.01	403.89 ± 4.61	
	6	0.103 ± 0.001	0.363 ± 0.014	6.85 ± 0.01	403.33 ± 5.96	
0.78 % TH	0	0.131 ± 0.006	0.417 ± 0.014	6.74 ± 0.09	427.67 ± 6.95	No
	1	0.118 ± 0.023	0.372 ± 0.002	6.71 ± 0.02	424.56 ± 4.01	
	3	0.112 ± 0.001	0.353 ± 0.010	6.72 ± 0.05	423.33 ± 3.72	
	6	0.112 ± 0.001	0.347 ± 0.014	6.73 ± 0/03	422.67 ± 1.37	
1.56 % TH	0	0.139 ± 0.005	0.420 ± 0.009	6.57 ± 0.10	468.00 ± 8.62	No
	1	0.123 ± 0.005	0.397 ± 0.023	6.46 ± 0.02	460.78 ± 3.67	
	3	0.121 ± 0.031	0.392 ± 0.006	6.41 ± 0.09	457.67 ± 0.52	
	6	0.102 ± 0.002	0.360 ± 0.015	6.40 ± 0.09	456.67 ± 1.86	
3.12 % TH	0	0.161 ± 0.004	0.467 ± 0.014	6.41 ± 0.02	495.00 ± 3.22	No
	1	0.150 ± 0.031	0.459 ± 0.004	6.44 ± 0.07	492.33 ± 1.99	
	3	0.146 ± 0.001	0.456 ± 0.021	6.45 ± 0.10	491.33 ± 1.37	
	6	0.144 ± 0.001	0.453 ± 0.014	6.45 ± 0.04	490.67 ± 1.37	

^a There is no significant difference observed for all parameters. TH – *Tualang* honey, TH-loaded patch – *Tualang* honey-loaded patch, SD – standard deviation.

Meanwhile, when POF cells were exposed to starch, there was a slight increase in the percentage of viability compared to the control group, as shown in Fig. 5b. After 24 hours of incubation, the rate of viability increased from 101.482 ± 7.735 % to 111.060 ± 10.018 % when exposed to concentrations of 0.09–50 % starch. A similar range of concentrations

also showed the same effect after 48 hours of exposure, with percentage viability ranging from 103.808 ± 8.120 % to 112.012 ± 8.932 %. In 72 hours of exposure, only concentrations of 0.19 % to 3.12 % starch showed viability above 100 %, with values of 101.102 ± 10.466 % to 125.324 ± 8.673 %. As for 100 % starch, the percentage viability drops drastically at the three-time interval, indicating that an inhibitory effect might be due to the high saturated solution.

Based on both results in Fig. 5a, several TH concentrations, such as 0.19, 0.39, 0.78, 1.56 and 3.12 %, were selected for loading into the patch formulation. While the selection of 5 % starch concentration in the formulation that based on previous study also falls in safer range to be used on POF cells (Fig. 5b). Fig. 5c showed that exposure with placebo patches slightly increased the percentage viability of POF cells particularly after 48- and significantly increase ($p < 0.05$) at 72-hours incubation time with value of 140.753 ± 0.531 % and 144.814 ± 0.749 % respectively compared to control group. This increased pattern persisted, along with the increased TH exposure, with values ranging from 145.154 ± 0.383 % to 165.077 ± 0.295 % for 48-hour incubation periods and from 148.817 ± 0.482 % to 197.264 ± 0.434 % for 72-hour incubation periods. For 48-hour incubation, compared with the placebo patch group (140.753 ± 0.531 %), TH-loaded patches with 1.56 % and 3.12 % TH showed the highest viability, with values of 165.077 ± 0.157 % and 165.077 ± 0.295 %, respectively. After 72 hours of incubation, TH-loaded patches with a concentration of 3.12 % TH showed the significantly highest percentage ($p < 0.05$) at 197.264 ± 0.434 %, compared to the placebo patch group (144.814 ± 0.749 %).

From the data, TH at concentrations below 0.78 % exhibited a proliferative effect, while concentrations above that level inhibited monolayer POF cells. This is consistent with previous studies, in which TH at concentrations below 1.0 % (approximately 0.02 %), were safe for the growth of the primary murine epidermal keratinocyte cell line (PAM212) and human periodontal ligament fibroblast (HPDLF) cells (52, 53). This was further demonstrated in this study by the cytotoxicity of oral patches, whereby both placebo and *Tualang* honey (TH)-loaded formulations exhibited cell viability above 70 %, indicating their biocompatibility and non-toxicity, as per ISO 10993-5 guidelines (54).

Contrary to the result of 3.12 % TH directly treated with POF, the combination of TH in TH-loaded patches, particularly at concentration 3.12 %, showed higher cell viability at 48 and 72 hours compared to other TH concentrations. Since the 3.12 % TH concentration falls beyond the range of proliferative effect of TH, the popular explanation might be that the interaction of direct TH, especially at concentrations above 0.78 %, supplies an immediate burst effect of full-spectrum bioactive components inside the honey that can create a high osmolarity, leading to an unsuitable environment for cell growth (55, 56). In contrast, the eluate from TH-loaded patches contains only the fraction of honey that leaches from the patch matrix and is often diluted by the polymer mixture (57). Moreover, the data suggested that the addition of TH to TH-loaded patches enables sustained, controlled release of the treatment over a more extended period, as the TH is encapsulated or embedded within a polymeric matrix. A similar pattern was found in previous studies wherein the addition of honey inside chitosan/gelatin/PVA and chitosan/PVA hydrogel films can sustain the biocompatibility up to 14 and 30 days when exposed to human fibroblast and normal human dermal fibroblast (NHDF) cells, respectively, without affecting the cell activities (10, 51).

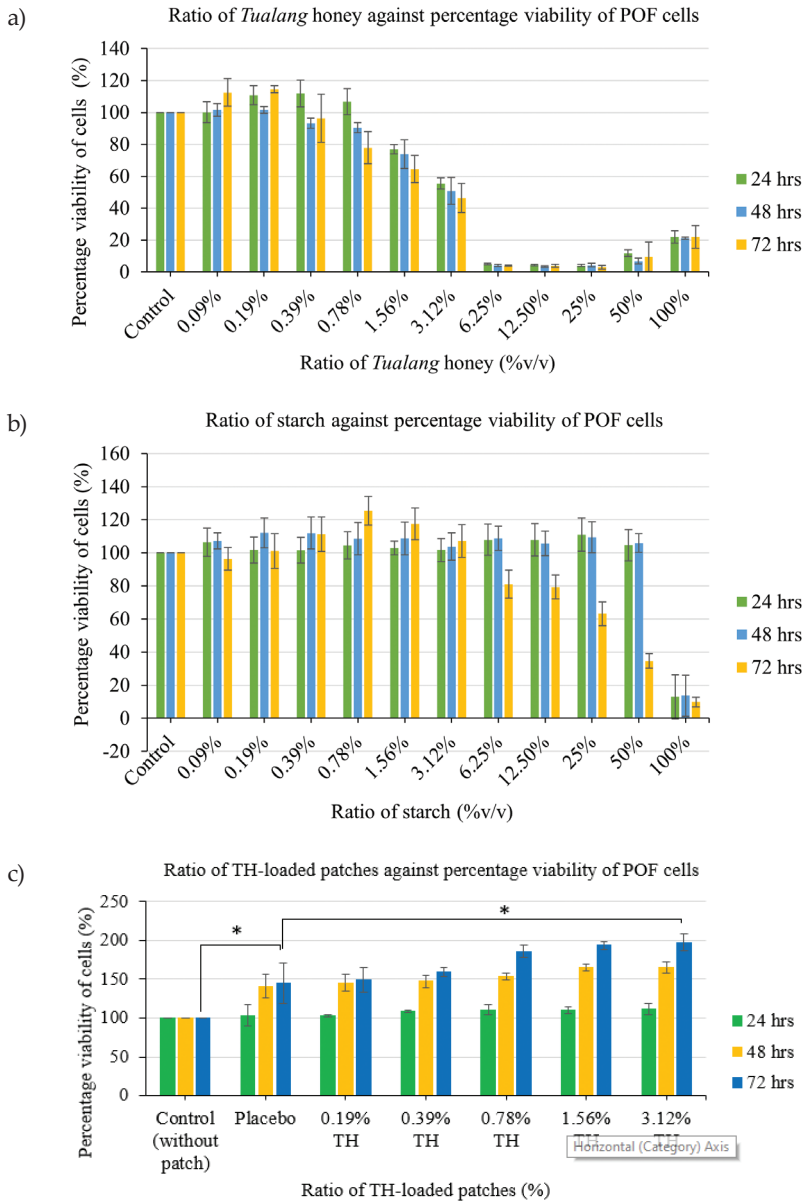


Fig. 5. Cell viability assay: a) various TH concentrations; b) various starch concentrations; c) placebo and TH-loaded patches (0.19, 0.39, 0.78, 1.56 and 3.12 %) against POF cells using MTT assay. Data are presented as the mean \pm SD from three independent experiments. Each was performed in triplicate, and $p < 0.05$ was considered significant compared to the control group (TH – *Tualang* honey, POF – primary oral fibroblasts, SD – standard deviation, MTT – 3-(4,5-dimethylthiazolyl-2)-2,5-diphenyltetrazolium bromide).

In vitro wound closure mechanism of oral patches

Since POF cell viability was higher with 3.12 % TH-loaded patches, this concentration was chosen as the optimal for the patches to undergo wound closure analysis. In this analysis, wound closure rate was expressed as a percentage of wound closure based on the average multiple horizontal measurement reduction across the wound area, recorded at 0, 24, 48, and 72 h. As shown in Fig. 6, the percentage of wound closure for POF were increased when treated with placebo patches with percentage value of $47.15 \pm 4.26\%$, $63.25 \pm 6.57\%$, and $77.56 \pm 7.67\%$, for 24, 48, and 72 hours, respectively compared to control group ($37.09 \pm 5.35\%$, $57.02 \pm 4.82\%$, and $74.55 \pm 6.65\%$). Meanwhile, 3.12 % TH-loaded patches resulted in slightly higher percentage wound closure than placebo and control group with the value of $57.09 \pm 5.34\%$, $73.71 \pm 4.17\%$, and $87.02 \pm 4.60\%$, respectively for time intervals of 24, 48, and 72 hours, indicating the gap width of the wound closed rapidly as the presence of TH enhance the proliferation of POF cells inside the culture.

Based on the result, the incorporation of TH into oral patches enhanced wound healing, cell migration, and proliferation, suggesting an active role in accelerating tissue repair. These findings are consistent with a previous study, in which honey-based biomaterials significantly promoted fibroblast migration due to the presence of bioactive sugars and phenolic compounds (34). Besides, honey has been reported to contain antioxidant compounds and natural sugars that play a crucial role in stimulating cell growth and ECM

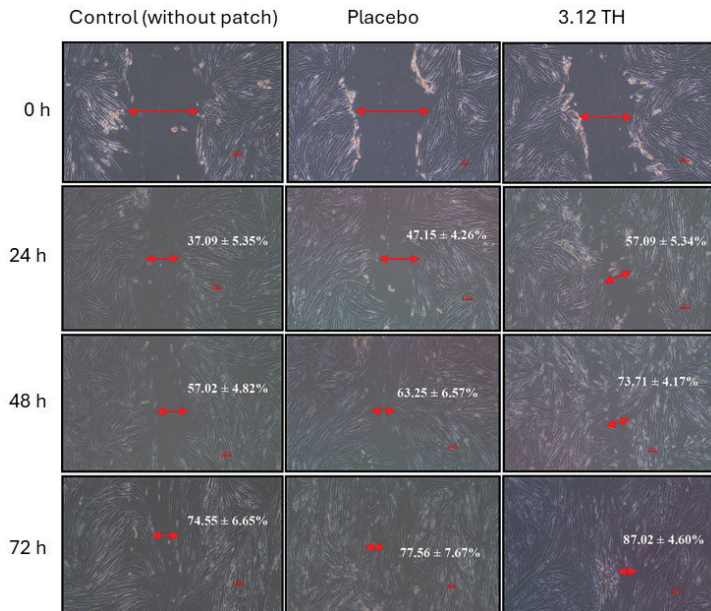


Fig. 6. Placebo and TH-loaded patches (3.12 %) were tested for wound healing properties of POF cells using the scratch assay protocol. Data are presented as the mean \pm SD from three independent experiments. Each was performed in triplicate, and $p < 0.05$ was considered significant compared to the control group (TH – Tualang honey, POF – primary oral fibroblasts, SD – standard deviation).

formation (10). Similar findings were reported in previous research, where honey-incorporated biomaterials improved fibroblast growth due to the presence of sugars that serve as an energy source for cell metabolism (51). This suggests that honey's bioactive compounds, including flavonoids and phenolic acids, contributed to enhanced cell proliferation.

CONCLUSIONS

The successful incorporation of *Tualang* honey (TH) into PVA-sago starch matrix demonstrated a stable and reproducible formulation for oral wound management. The addition of TH did not compromise the physicochemical integrity, mechanical strength, or stability of the patches over six months of storage, confirming the sturdiness of the formulation. Notably, incorporating TH, particularly at concentrations of 3.12 % or lower, enhanced physicochemical and mechanical properties, including swelling capacity, flexibility, as well as biological performance, leading to improved primary oral fibroblasts proliferation and accelerated wound closure. Overall, these findings highlight that TH functions not only as a bioactive agent but also as an enhancer within the polymeric matrix. In conclusion, this study proposes TH-loaded oral patches as a structurally stable, biologically active, and clinically translatable platform for promoting oral mucosal cell regeneration.

Abbreviations and acronyms. – DDS – drug delivery system; DMEM – Dulbecco's Modified Eagle's Medium; DMSO – dimethyl sulfoxide; ECM – extracellular matrix; MTT – 3-(4,5-dimethylthiazolyl-2)-2,5-diphenyltetrazolium bromide; NDDS – novelty drug delivery system; OD – optical density; POF – primary oral fibroblasts; PVA – polyvinyl alcohol; SD – standard deviation; SEM – scanning electron microscopy; TH – *Tualang* honey; TH-loaded patches – *Tualang* honey-loaded patches.

Acknowledgements. – The authors would like to express their gratitude to University Sains Islam Malaysia (USIM) and the Ministry of Higher Education (MoHE), Malaysia, for the funding provided for this research.

Conflict of interests. – The authors did not experience any conflict of interest throughout this research.

Funding. – This work was supported by the Ministry of Higher Education (MOHE) of Malaysia under the Fundamental Research Grant Scheme (FRGS) with reference number FRGS/1/2020/STG05/USIM/03/1.

Author's contribution. – Conceptualisation, S.N.N.Y, N.I.M., Z.S., N.H., N.A.M., M.S.A. and M.R.M.I.; writing, preparing the original draft, S.N.N.Y, N.I.M., Z.S., N.H., N.A.M. and M.R.M.I.; writing, review and editing, S.N.N.Y, N.I.M., Z.S., N.H., N.A.M., M.S.A. and M.R.M.I.; supervision and funding acquisition, Z.S. All authors have read, reviewed, and reached an agreement on the published version of the manuscript.

REFERENCES

1. M. Waasdorp, B. P. Krom, F. J. Bikker, P. P. M. van Zuijlen, F. B. Niessen and S. Gibbs, The bigger picture: Why oral mucosa heals better than skin, *Biomolecules* 11(8) (2021) Article ID 1165 (22 pages); <https://doi.org/10.3390/BIOM11081165>
2. J. E. Glim, M. V. Egmond, F. B. Niessen, V. Everts and R. H. J. Beelen, Detrimental dermal wound healing: What can we learn from the oral mucosa?, *Wound Repair and Regeneration* 21(5) (2013) 648–660; <https://doi.org/10.1111/WRR.12072>

3. X. Lei, L. Cheng, H. Lin, M. Pang, Z. Yao, C. Chen, T. Forouzanfar, F. J. Bikker, G. Wu and B. Cheng, Human salivary histatin-1 is more efficacious in promoting acute skin wound healing than acellular dermal matrix paste, *Front. Bioeng. Biotechnol.* **8**(1) (2020) Article ID 999 (12 pages); <https://doi.org/10.3389/FBIOE.2020.00999>
4. M. Hao, D. Wang, M. Duan, S. Kan, S. Li, H. Wu, J. Xiang and W. Liu, Functional drug-delivery hydrogels for oral and maxillofacial wound healing, *Front. Bioeng. Biotechnol.* **11**(1) (2023) Article ID 1241660 (18 pages); <https://doi.org/10.3389/FBIOE.2023.1241660>
5. H. M. A. Al-Azzawi, R. Paolini and A. Celentano, Is hydrogel an appropriate bioadhesive material for sutureless oral wound closure?, *Health Sci. Rep.* **7**(12) (2024) Article ID 70249 (7 pages); <https://doi.org/10.1002/HSR2.70249>
6. K. K. Jain, An overview of drug delivery systems, *MIMB* **2059**(1) (2019) 1–54; https://doi.org/10.1007/978-1-4939-9798-5_1
7. M. Ikram, N. Gilhotra and R. M. Gilhotra, Formulation and optimisation of mucoadhesive buccal patches of losartan potassium by using response surface methodology, *Adv. Biomed. Res.* **4**(1) (2015) 239–252; <https://doi.org/10.4103%2F2277-9175.168606>
8. N. H. Thang, T. B. Chien and D. X. Cuong, Polymer-based hydrogels applied in drug delivery: An overview, *Gels* **9**(7) (2023) Article ID 523 (38 pages); <https://doi.org/10.3390/gels9070523>
9. T. C. Ezike, U. S. Okpala, U. L. Onoja, C. P. Nwike, E. C. Ezeako, O. J. Okpara, C. C. Okoroafor, S. C. Eze, O. L. Kalu, E. C. Odoh, U. G. Nwadike, J. O. Ogbodo, B. U. Umeh, E. C. Ossai and B. C. Nwanguma, Advances in drug delivery systems, challenges and future directions, *Heliyon* **9**(6) (2023) Article ID 17488 (17 pages); <https://doi.org/10.1016/j.heliyon.2023.e17488>
10. A. Shamloo, Z. Aghababaie, H. Afjoul, M. Jami, M. R. Bidgoli, M. Vossoughi, A. Ramazani and K. Kamyabhesari, Fabrication and evaluation of chitosan/gelatin/PVA hydrogel incorporating honey for wound healing applications: An in vitro, in vivo study, *Int. J. Pharm.* **592**(1) (2021) Article ID 120068 (29 pages); <https://doi.org/10.1016/j.ijpharm.2020.120068>
11. M. H. Norahan, S. C. Pedroza-González, M. G. Sánchez-Salazar, M. M. Álvarez and G. T. D. Santiago, Structural and biological engineering of 3D hydrogels for wound healing, *Bioact. Mater.* **24**(1) (2023) 197–235; <https://doi.org/10.1016%2Fj.bioactmat.2022.11.019>
12. J. Su, J. Li, J. Liang, K. Zhang and J. Li, Hydrogel preparation methods and biomaterials for wound dressing, *Life* **11**(10) (2021) Article ID 1016 (22 pages); <https://doi.org/10.3390%2F11101016>
13. D. Taylan, İ. Güneş, E. Durukan and Ö. Gök, Characterisation of hybrid hydrogels combining natural polymers, *BioRxiv* **1**(1) (2023) Article ID 556716 (9 pages); <https://doi.org/10.1101/2023.09.07.556716>
14. S. Ahmed, S. A. Sulaiman, A. A. Baig, M. Ibrahim, S. Liaqat, S. Fatima, S. Jabeen, N. Shamim and N. H. Othman, Honey as a potential natural antioxidant medicine: An insight into its molecular mechanisms of action, *Oxidative Medicine and Cellular Longevity* **2018**(1) (2018) Article ID 8367846 (19 pages); <https://doi.org/10.1155%2F2018%2F8367846>
15. K. Devasvaran, J. J. Tan, C. T. Ng, L. Y. Fong and Y. K. Yong, Malaysian *Tualang* honey inhibits hydrogen peroxide-induced endothelial hyperpermeability, *Oxidative Medicine and Cellular Longevity* **2019**(1) (2019) Article ID 1202676 (10 pages); <https://doi.org/10.1155/2019/1202676>
16. R. Angioi, A. Morrin and B. White, The rediscovery of honey for skin repair: Recent advances in mechanisms for honey-mediated wound healing and scaffolded application techniques, *Appl. Sci.* **11**(11) (2021) Article ID 5192 (27 pages); <https://doi.org/10.3390/app11115192>
17. A. Z. K. Lo, S. K. Lukman, C. H. Lai, N. M. Zain and S. Saidin, Stingless bee honey incorporated cellulose hydrogel/poly(lactic-co-glycolic acid) patch as an alternative treatment for aphthous stomatitis, *Cellulose Chem. Technol.* **55**(5–6) (2020) 539–603; <http://dx.doi.org/10.35812/CelluloseChemTechnol.2021.55.48>
18. H. P. S. A. Khalil, S. Muhammad, E. B. Yahya, L. K. M. Amanda, S. A. Bakar, C. K. Abdullah, A. R. Aiman, M. Marwan and S. Rizal, Synthesis and characterization of novel patchouli essential oil

- loaded starch-based hydrogel, *Gels* **8**(9) (2022) Article ID 536 (16 pages); <https://doi.org/10.3390/GELS8090536>
19. C. L. P. Gutiérrez, F. Cottone, C. Pagano, A. D. Michele, D. Puglia, F. Luzi, F. Dominici, R. Sinisi, M. Ricci, C. A. V. Iborra and L. Perioli, The optimisation of pressure-assisted microsyringe (PAM) 3D printing parameters for the development of sustainable starch-based patches, *Polymers* **15**(18) (2023) Article ID 3792 (19 pages); <https://doi.org/10.3390/POLYM15183792>
 20. R. F. El-Kased, R. I. Amer, D. Attia and M. M. Elmazar, Honey-based hydrogel: In vitro and comparative in vivo evaluation for burn wound healing, *Sci. Rep.* **7**(1) (2017) Article ID 9692 (11 pages); <https://doi.org/10.1038/s41598-017-08771-8>
 21. J. Sringam, P. Pankongadisak, T. Trongsatitkul and N. Suppakarn, Improving mechanical properties of starch-based hydrogels using double network strategy, *Polymers* **14**(17) (2022) Article ID 3552 (18 pages); <https://doi.org/10.3390/POLYM14173552>
 22. F. F. Hilmi, M. U. Wahit, N. A. Shukri, Z. Ghazali and A. Z. Zanuri, Physico-chemical properties of biodegradable films of polyvinyl alcohol/sago starch for food packaging, *Materials Today: Proceedings* **16**(4) (2019) 1819–1824; <https://doi.org/10.1016/j.matpr.2019.06.056>
 23. G. Aydin and E. B. Zorlu, Characterisation and antibacterial properties of novel biodegradable films based on alginate and roselle (*Hibiscus sabdarifa* L.) extract, *Waste and Biomass Valorization* **13**(1) (2022) 2991–3002; <https://doi.org/10.1007/s12649-022-01710-3>
 24. G. P. Ribeiro, J. K. Villas-Bôas, W. A. Spinosa and S. H. Prudencio, Influence of freezing, pasteurization and maturation on *Tiúba* honey quality, *LWT* **90**(1) (2018) 607–612; <https://doi.org/10.1016/J.LWT.2017.12.072>
 25. E. Özakar, R. Sevinç-Özakar and B. Yilmaz, Preparation, Characterisation, and evaluation of cytotoxicity of fast dissolving hydrogel based oral thin films containing pregabalin and methylcobalamin, *Gels* **9**(2) (2023) Article ID 147 (29 pages); <https://doi.org/10.3390/gels9020147>
 26. R. N. Wenzel, Surface roughness and contact angle, *J. Phys. Chem.* **53**(9) (1949) 1466–1467; <https://doi.org/10.1021/J150474A015>
 27. S. Wang, P. Yu, X. Li, Z. Zhao, Y. Dong and X. Li, Design and fabrication of functional hydrogels with specific surface wettability, *Colloid and Interface Sci. Comm.* **52**(1) (2023) Article ID 100697 (14 pages); <https://doi.org/10.1016/J.COLCOM.2023.100697>
 28. D. Chelminiak-Dudkiewicz, A. Smolarkiewicz-Wyczachowski, K. Mylkie, M. Wujak, D. T. Mlynarczyk, P. Nowak, S. Bocian, T. Goslinski and M. Ziegler-Borowska, Chitosan-based films with cannabis oil as a base material for wound dressing application, *Sci. Rep.* **12**(1) (2022) Article ID 18658 (16 pages); <https://doi.org/10.1038/s41598-022-23506-0>
 29. M. U. A. Khan, G. M. Stojanović, R. Hassan, T. J. S. Anand, M. Al-Ejji and A. Hasan, Role of graphene oxide in bacterial cellulose-gelatin hydrogels for wound dressing applications, *ACS Omega* **8**(18) (2023) 15909–15919; <https://doi.org/10.1021/ACSOMEGA.2C07279>
 30. B. Singh, J. Singh, V. Sharma, P. Sharma and R. Kumar, Functionalization of bioactive moringa gum for designing hydrogel wound dressings, *Hybrid Adv.* **4**(1) (2023) Article ID 100096 (15 pages); <https://doi.org/10.1016/J.HYBADV.2023.100096>
 31. R. Krishnan, T. Mohammed, G. S. Kumar and A. SH, Honey crystallization: Mechanism, evaluation, and application, *Pharm. Innov. J.* **10**(5S) (2021) 222–231; <https://doi.org/10.22271/TPI.2021.V10.I5SD.6213>
 32. Y. Yang, J. Fu, Q. Duan, H. Xie, X. Dong and L. Yu, Strategies and methodologies for improving toughness of starch films, *Foods* **13**(24) (2024) Article ID 4036 (31 pages); <https://doi.org/10.3390/FOODS13244036>
 33. F. G. Prezotti, I. Siedle, F. I. Boni, M. Chorilli, I. Müller and B. S. F. Cury, Mucoadhesive films based on gellan gum/pectin blends as potential platform for buccal drug delivery, *Pharm. Devel. Technol.* **25**(2) (2019) 159–167; <https://doi.org/10.1080/10837450.2019.1682608>

34. A. Brites, M. Ferreira, S. Bom, L. Grenho, R. Claudio, P. S. Gomes, M. H. Fernandes, J. Marto and C. Santos, Fabrication of antibacterial and biocompatible 3D printed manuka-gelatin based patch for wound healing applications, *Int. J. Pharm.* **632**(1) (2023) Article ID 122541 (12 pages); <https://doi.org/10.1016/J.IJPHARM.2022.122541>
35. R. Sharma, S. Kamboj, G. Singh and V. Rana, Development of aprepitant loaded orally disintegrating films for enhanced pharmacokinetic performance, *Eur. J. Pharm. Sci.* **84**(1) (2016) 55–69; <https://doi.org/10.1016/J.EJPS.2016.01.006>
36. M. J. Kim, W. B. Lee and D. H. Park, Comparison of the effect of silicone gel sheets by thickness on excisional scars in pediatric and adolescent patients, *Arch. Aesthetic Plast. Surg.* **28**(1) (2022) 17–23; <https://doi.org/10.14730/AAPS.2021.00339>
37. A. Tijani, P. Dogra, M. J. Peláez, Z. Wang, V. Cristini and A. Puri, Mechanistic modeling-guided optimization of microneedle-based skin patch for rapid transdermal delivery of naloxone for opioid overdose treatment, *Drug Del. Transl. Res.* **13**(1) (2022) 320–338; <https://doi.org/10.1007/S13346-022-01202-W>
38. S. Ahmed and N. H. Othman, Review of the medicinal effects of *Tualang* honey and a comparison with Manuka honey, *Malays. J. Med. Sci.* **20**(3) (2013) 6–13; <https://pubmed.ncbi.nlm.nih.gov/articles/PMC3743976/>
39. R. M. Zohdi, Z. A. B. Zakaria, N. Yusof, N. M. Mustapha and M. N. H. Abdullah, Gelam (*Melaleuca* spp.) honey-based hydrogel as burn wound dressing, *Evidence-Based Complement. Alter. Med.* **12**(1) (2011) Article ID 843025 (7 pages); <https://doi.org/10.1155/2012/843025>
40. S. Frothingham, What is the pH of saliva?, *Healthline*, September 2018; <https://www.healthline.com/health/ph-of-saliva>; last access date April 15, 2025
41. E. G. Andriotis, G. K. Eleftheriadis, C. Karavasili and D. G. Fatouros, Development of bioactive patches based on pectin for the treatment of ulcers and wounds using 3D-bioprinting technology, *Pharmaceutics* **12**(1) (2020) Article ID 56 (24 pages); <https://doi.org/10.3390/pharmaceutics12010056>
42. P. Pająk, D. Gałkowska, L. Juszczyk and G. Khachatryan, Octenyl succinylated potato starch-based film reinforced by honey-bee products: Structural and functional properties, *Food Packaging and Shelf Life* **34**(1) (2022) Article ID 100995; <https://doi.org/10.1016/J.FPSL.2022.100995>
43. N. A. N. M. Azam and K. A. M. Amin, Influence of Manuka honey on mechanical performance and swelling behaviour of alginate hydrogel film, *IOP Conf. Ser.: Mater. Sci. Eng.* **440**(1) (2018) Article ID 012024 (7 pages); <https://doi.org/10.1088/1757-899X/440/1/012024>
44. Z. Żołek-Tryznowska and Ł. Cichy, Glycerol derivatives as a modern plasticizers for starch films, 9th *International Symposium on Graphic Engineering and Design* **1**(1) (2018) 217–222; <https://doi.org/10.24867/GRID-2018-P27>
45. D. S. Perwitasari, N. A. Fauziyah, R. H. Pesra and N. L. Putu, Preliminary study of synthesis and characterisation of biodegradable avocado seed starch-chitosan plastic with glycerol plasticizer, *BioResources* **19**(4) (2024) 8769–8780; <https://doi.org/10.15376/BIORES.19.4.8769-8780>
46. M. B. Stie, J. R. Gätke, F. Wan, I. S. Chronakis, J. Jacobsen and H. M. Nielsen, Swelling of mucoadhesive electrospun chitosan/polyethylene oxide nanofibers facilitate adhesion to the sublingual mucosa, *Carbohydr. Polym.* **242**(1) (2020) Article ID 116428 (29 pages); <https://doi.org/10.1016/J.CARB-POL.2020.116428>
47. F. Bisotti, F. Pizzetti, G. Storti and F. Rossi, Mathematical modelling of cross-linked polyacrylic-based hydrogels: Physical properties and drug delivery, *Drug Deliv. Translat. Res.* **12**(1) (2022) 1928–1942; <https://doi.org/10.1007/S13346-022-01129-2>
48. W. Feng and Z. Wang, Tailoring the swelling-shrinkable behavior of hydrogels for biomedical applications, *Adv. Sci.* **10**(28) (2023) Article ID 2303326 (41 pages); <https://doi.org/10.1002/ADVS.202303326>
49. M. D. Mandal and S. Mandal, Honey: Its medicinal property and antibacterial activity, *Asian Pacific J. Trop. Biomed.* **1**(2) (2011) 154–160; [https://doi.org/10.1016/S2221-1691\(11\)60016-6](https://doi.org/10.1016/S2221-1691(11)60016-6)

50. H. Hadi, S. Omar and A. Awadh, Honey, a gift from nature to health and beauty: A review, *Brit. J. Pharm.* **1**(1) (2016) 46–54; <https://doi.org/10.5920/BJPHARM.2016.05>
51. M. Koosha, H. Aalipour, M. J. S. Shirazi, A. Jebali, H. Chi, S. Hamed, N. Wang, T. Li and H. Moravvej, Physically crosslinked chitosan/PVA hydrogels containing honey and allantoin with long-term biocompatibility for skin wound repair: An in vitro and in vivo study, *J. Funct. Biomater.* **12**(4) (2021) Article ID 61 (19 pages); <https://doi.org/10.3390/JFB12040061>
52. I. Ahmad, H. Jimenez, N. S. Yaacob and N. Yusuf, Tualang honey protects keratinocytes from ultraviolet radiation-induced inflammation and DNA damage, *Photochem. Photobiol.* **88**(5) (2012) 1198–1204; <https://doi.org/10.1111/J.1751-1097.2012.01100.X>
53. L. X. Yu, H. Taib, Z. Berahim, A. Ahmad and S. L. A. Zainuddin, The effect of Tualang honey on human periodontal ligament fibroblast proliferation and alkaline phosphatase level, *Sains Malaysiana* **44**(7) (2015) 1021–1025; <https://doi.org/10.17576/JSM-2015-4407-14>
54. P. Pal, H. Li, R. Al-Ajeil, A. K. Mohammed, A. Rezk, G. Melinte, A. Nayfeh, D. Shetty and N. El-Atab, Energy efficient memristor based on green-synthesised 2D carbonyl-decorated organic polymer and application in image denoising and edge detection: Toward sustainable AI, *Adv. Sci.* **11**(45) (2024) Article ID 2408648 (9 pages); <https://doi.org/10.1002/ADVS.202408648>
55. S. Almasaudi, The antibacterial activities of honey, *Saudi J. Biol. Sci.* **28**(4) (2021) 2188–2196; <https://doi.org/10.1016/J.SJBS.2020.10.017>
56. M. L. Hossain, L. Y. Lim, K. Hammer, D. Hettiarachchi and C. Locher, A review of commonly used methodologies for assessing the antibacterial activity of honey and honey products, *Antibiotics* **11**(7) (2022) Article ID 975 (17 pages); <https://doi.org/10.3390/ANTIBIOTICS11070975>
57. S. A. Abraham, G. Yashavanth, R. Deveswaran, S. Bharath, M. Azamathulla and S. Shanmuganathan, Honey based hydrogel as delivery system for wound healing, *Materials Today: Proceedings* **49**(5) (2022) 1709–1718; <https://doi.org/10.1016/J.MATPR.2021.07.488>